Clinical Cancer Research

Activation of *EZH2* and *SUZ12* Regulated by E2F1 Predicts the Disease Progression and Aggressive Characteristics of Bladder Cancer

Se-Ra Lee[1], Yun-Gil Roh[1], Seon-Kyu Kim[2], Ju-Seog Lee[3], So-Young Seol[1], Hyun-Hee Lee[1], Won-Tae Kim[1], Wun-Jae Kim[4], Jeonghoon Heo[5], Hee-Jae Cha[6], Tae-Hong Kang[1], Jin Woong Chung[1], In-Sun Chu[2], and Sun-Hee Leem[1]

Abstract

Purpose: Previous study identified *E2F1* as a key mediator of non–muscle-invasive bladder cancer (NMIBC) progression. The aim of this study was to identify the *E2F1*-related genes associated with poor prognosis and aggressive characteristics of bladder cancer.

Experimental Design: Microarray analysis was performed to find *E2F1*-related genes associated with tumor progression and aggressiveness in the gene expression data from 165 primary patients with bladder cancer. The biologic activity of *E2F1*-related genes in tumor progression and aggressiveness was confirmed with experimental assays using bladder cancer cells and tumor xenograft assay.

Results: The expression of *E2F1* was significantly associated with *EZH2* and *SUZ12*. The overexpression of *E2F1*, *EZH2*, and *SUZ12* enhanced cancer progression including cell colony formation, migration, and invasiveness. Knockdown of these genes reduced motility, blocked invasion, and decreased tumor size *in vivo*. E2F1 bound the proximal *EZH2* and *SUZ12* promoter to activate transcription, suggesting that *E2F1* and its downstream effectors, *EZH2* and *SUZ12*, could be important mediators for the cancer progression. In addition, we confirmed an association between these genes and aggressive characteristics. Interestingly, the treatment of anticancer drugs to the cells overexpressing *E2F1*, *EZH2*, and *SUZ12* induced the expression of *CD44*, *KLF4*, *OCT4*, and *ABCG2* known as cancer stem cell (CSC)–related genes.

Conclusions: The link between *E2F1*, *EZH2*, and/or *SUZ12* revealed that E2f1 directly regulates transcription of the *EZH2* and *SUZ12* genes. The signature of *E2F1--EZH2--SUZ12* shows a predictive value for prognosis in bladder tumors and the *E2F1–EZH2–SUZ12*–driven transcriptional events may regulate the cancer aggressiveness and chemo-resistance, which may provide opportunity for development of new treatment modalities. *Clin Cancer Res; 21(23); 5391–403. ©2015 AACR.*

Introduction

Bladder cancer is the sixth most common cancer in men and women populations. In 2013, 72,570 new cases of bladder cancer were diagnosed and 15,210 deaths were due to bladder cancer in the United States (1). This cancer is characterized by 2 histologically distinct subtypes: non–muscle-invasive bladder cancer (NMIBC) and muscle-invasive bladder cancer (MIBC) at initial diagnosis (2). NMIBC is a heterogeneous disease (3), and patients frequently experience disease recurrence and 10% to 30% of them progress to MIBC, which is responsible for most bladder cancer–specific deaths (2). Because MIBC frequently leads to distant metastases (4), a major focus of research has been to understand the mechanisms that promote cancer progression. Although there have been many efforts to construct a robust model to predict progression of NMIBC using clinical information and pathologic classification (3, 5–7), precisely predicting the behavior of heterogeneous NMIBC remains challenging.

Previously, our genome-wide gene expression profile study using microarray technologies successfully identified a gene expression signature that could predict the likelihood of progression of NMIBC (8). Expression of *E2F1* was significantly upregulated in the MIBC subtype, strongly indicating that activation of *E2F1* might be a critical genetic event in the development of or progression to MIBC (8). Because *E2F1* was not uniformly absent in all NMIBCs, we re-examined expression of *E2F1* in NMIBCs and subdivided the patients into 2 groups according to the expression level of *E2F1*. The progression rate in the *E2F1*-high groups was profoundly higher than in the *E2F1*-low group, showing that *E2F1* is strongly associated with NMIBC-to-MIBC progression (8).

[1]Department of Biological Science, Dong-A University, Busan, Republic of Korea. [2]Korean Bioinformation Center, Korea Research Institute of Bioscience and Biotechnology, Daejeon, Republic of Korea. [3]Department of Systems Biology, Division of Cancer Medicine, University of Texas MD Anderson Cancer Center, Houston, Texas. [4]Department of Urology, College of Medicine, Chungbuk National University, Cheongju, Republic of Korea. [5]Departments of Molecular Biology and Immunology, College of Medicine, Kosin University, Busan, Republic of Korea. [6]Departments of Parasitology and Genetics, Kosin University College of Medicine, Busan, Republic of Korea.

Note: Supplementary data for this article are available at Clinical Cancer Research Online (http://clincancerres.aacrjournals.org/).

S.-R. Lee and Y.-G. Roh contributed equally to this article.

Corresponding Authors: Sun-Hee Leem, Department of Biological Science, College of Natural Science, Dong-A University, Busan, 604–714, Republic of Korea. Phone: 82-51-200-5639; Fax: 82-51-200-7269; E-mail: shleem@dau.ac.kr; and In-Sun Chu, Korean Bioinformation Center, Korea Research Institute of Bioscience and Biotechnology, Daejeon, 305-806, Republic of Korea. Phone: 82-42-879-8520; Fax: 82-42-879-8519; E-mail: chu@kribb.re.kr

doi: 10.1158/1078-0432.CCR-14-2680

Translational Relevance

Non–muscle-invasive bladder cancer (NMIBC) accounts for 80% of bladder cancers, 20% of which experience the progression into muscle-invasive bladder cancer (MIBC) that is responsible for the most cancer-specific deaths. In this study, the activation of *E2F1–EZH2–SUZ12* signature was strongly associated with NMIBC-to-MIBC progression. The signature to discriminate distinct molecular subgroups of NMIBC was developed in a training cohort of from 165 patients with bladder cancer and validated in independent cohort. Moreover, we examined *E2F1* downstream pathway mediating NMIBC progression and illustrated an association between the overexpression of *E2F1–EZH2–SUZ12* and chemoresistance. Thus, we suggest that the transcriptional changes of *E2F1–EZH2–SUZ12* clearly predict bladder cancer aggressiveness, as well as anticancer drug resistance. Identification of a high-risk subgroup of patients with NMIBC based on the *E2F1–EZH2–SUZ12* signature may improve the application of currently available treatments and provide opportunities for the development of new treatment modalities.

In this study, on the basis of gene-to-gene network analysis, we found that the expression levels of *EZH2* and *SUZ12*, binding partners of polycomb complex PRC2 (polycomb repressive complex 2) and direct targets of *E2F1*, were significantly higher in the *E2F1*-high subgroup than in the *E2F1*-low subgroup. Overexpression of several PcG proteins has been associated with many tumors and has also been identified as prognostic indicator in several tumors (9–13). The PRC2 core components are known such as EZH2, SUZ12, EED, and RBBP4 or RBBP7, which catalyze trimethylation of histone H3 lysine 27 (H3K27me3; ref. 14). Several studies reported that PRC2 was overexpressed in numerous cancer types and played a critical role in the aberrant silencing of tumor suppressor genes (15, 16).

Higher expression of the *EZH2* and *SUZ12* genes is clearly associated with tumor progression and overall survival (OS) in bladder cancer, but other genes including *EED* did not show significant level of prediction in this study. Therefore, we investigated the biologic activities of *EZH2* and *SUZ12*, whose expression was significantly associated with poor prognosis and reflected the aggressive characteristics of bladder cancer. Moreover, we examined these genes' downstream pathways to mediate NMIBC progression, illustrating that *E2F1* and *EZH2* activated cancer stem cell (CSC) signaling pathways in anticancer drug-treated environments. Thus, we suggest that the transcriptional changes of *E2F1*, *EZH2*, and *SUZ12* clearly predict bladder cancer aggressiveness, as well as anticancer drug resistance.

Materials and Methods

Cell culture

Human bladder cancer cell lines (EJ and 5637) were obtained from the ATCC. Other cell lines (UC5 and UC9) were provided by H. Barton Grossman (Department of Urology, University of Texas MD Anderson Cancer Center, Houston, TX: deposited into Public Health England, United Kingdom). The cells in this study were used within 6 months in our laboratory and were obtained from a cell bank that performed cell line characterizations. Cells from ATCC were certificated by the results of the short tandem repeat (STR) DNA profiling assay, cytochrome *c* oxidase I assay, and mycoplasma contamination assay. Eleven of UC series cells were characterized by the STR-PCR method and for mycoplasma contamination.

UC5, UC9 (NMIBC cells), and EJ (MIBC cells) were cultured in DMEM (Hyclone) supplemented with 10% FBS (Hyclone) and 1% penicillin/streptomycin (Hyclone). 5637 (MIBC) cells were cultured in RPMI-1640 medium (Hyclone).

Microarray gene expression profiling

We used a gene expression dataset (GSE13507, $n = 256$) containing 165 primary patients with bladder cancer in a previous study (8). Among the 165 cancers, 102 were histopathologically proven to be primary NMIBC and remained 63 were primary MIBC [GSE13507; the Korean cohort, $n = 165$ (102 NMIBCs and 63 MIBCs)]. Clinical data including progression-free survival (PFS), updated in January 2010, were obtained from the Chungbuk National University Hospital. To validate a prognostic value of the signature, 3 other gene expression datasets of patients with bladder cancer from hospitals of the Swedish southern healthcare region [GSE32894, $n = 308$ (215 NMIBCs and 93 MIBCs); ref. 17], Skane University Hospital [GSE32548, $n = 131$ (93 NMIBCs and 38 MIBCs); ref. 18], and University Hospital of Lund [GSE19915, $n = 146$ (97 NMIBCs and 49 MIBCs); ref. 19] were collected. Among them, MIBC data from GSE32894 and GSE32548 were combined, and a total of 58 MIBCs, whose survival time data were available, were used to assess survival rate of MIBC. Additional gene expression dataset including 19 bladder cancer cell lines was also examined in this study (GSE48277, $n = 349$). All gene expression datasets (GSE13507, GSE32894, GSE32548, GSE19915, and GSE48277) were freely available at NCBI GEO database.

To estimate prognostic values (PFS of NMIBC and OS of MIBC) of a signature combined with *E2F1*, *EZH2*, and *SUZ12* genes, we adopted a previously developed strategy using the Cox regression coefficient for the genes in the signature [prognostic index (PI); refs. 20, 21]. Additional analysis was carried out as described in Supplementary Methods S1. Gene network–based activation regulator analyses were performed using the Ingenuity Pathway Analysis (IPA) tool.

Plasmid construction and transfection

The plasmid construct was the pcDNA6-V5-His–tagged expression vector with fusion coding sequence (CDS) of *E2F1*, *EZH2*, and *SUZ12* (Invitrogen) genes. Transfection of plasmids was carried out using the jetPRIME reagent (Polyplus Transfection Inc.) at a ratio of DNA to jetPRIME of 1:3 according to the manufacturer's protocol. The measurement of gene expression at 24 hours posttransfection was normalized with the corresponding empty vectors.

RT-PCR and real-time PCR

The M-MLV Reverse Transcription kit (Beams Biotechnology) along with 3 μg of total RNA and poly(dT) primers were used for synthesis of cDNA. RT-PCR was carried out using an Emerald Amp GT PCR Master Mix (Takara Bio Inc.) to detect the mRNA level of *E2F1*, *EZH2*, and *SUZ12* with primer sets (in Supplementary Methods S2). PCR cycling conditions were 94°C for 2 minutes

to activate DNA polymerase, followed by 25 to 28 cycles of 94°C for 30 seconds, 58°C for 20 seconds, and 72°C for 40 seconds, and 72°C for 7 minutes for postelongation. Real-time PCR was carried out TOPreal premix SYBR Green (Enzynomics) and β-actin was used as control.

Western blot analysis

Proteins from the 5637, EJ, and UC5 cells were homogenized in RIPA buffer containing protease inhibitor (Roche), and the protein concentration was determined by using the BCA Assay (Thermo Scientific; ref. 22). The antibodies used in immunoblotting were against E2F1 (A300-766A, Bethyl Laboratories), EZH2 (4905, Cell Signaling Technology Inc.) SUZ12 (A302-407A, Bethyl Laboratories), and β-actin (4967, Cell Signaling Technology Inc.). Immunoreactivity was detected using the ECL Detection System (GE Healthcare BioSciences Corp.). Films were exposed at multiple time points to ensure that images were not saturated.

RNAi assay

siRNAs targeting *E2F1*, *EZH2*, and *SUZ12* were used: the SMARTpool ON-TARGET plus siE2F1 (L-003259-00; Dharmacon, GE Healthcare Bio-Sciences Corp.), siEZH2 (L-004218-00; Dharmacon), and siSUZ12 (L006957-00; Dharmacon). The SMARTpool ON-TARGET plus siControl nontargeting pool (D-001810-10) was purchased from Dharmacon. Cell were grown on 60-mm dishes and transfected either with control siRNA, siE2F1, siEZH2, or siSUZ12 (siRNA; 100 nmol/mL). The cells were analyzed 24 hours posttransfection.

We obtained shRNAs for *E2F1*, *EZH2*, and *SUZ12* from Sigma-Aldrich (MISSION shRNA). Each shRNA for *E2F1*, *EZH2*, or *SUZ12* was cloned into the pLKO.1-puro vector, using the Polymerase III U6-RNA promoter. A set of 5 shRNAs to each of *E2F1*, *EZH2*, and *SUZ12* was tested for knockdown, and the shRNA containing the sequences for *E2F1*, *EZH2*, and *SUZ12* was chosen for these experiments, because both mRNA and protein of E2f1, Ezh2, and Suz12 were effectively decreased. We used nontarget shRNA vector (Cat. No SHC016) as a control and selected stably expressing cells using puromycin (2 μg/mL).

MTT cell viability assay and soft-agar cologenic assay

Cell viability was detected using MTT assay. Cells were seeded in 96-well plates at a density of 1,000 cells per well, and then cells were incubated for 24 and 48 hours. Ten microliters of MTT (5 mg/mL; Sigma-Aldrich) was added to each well and incubated for 3 hours. At the end of the incubation, the supernatants were removed and 100 μL of dimethyl sulfoxide (Sigma-Aldrich) was added to each well, and absorbance at 490 nm was determined for each well using a Wallac Vector 1420 Multilabel Counter (EG&G Wallac). For each experimental condition, 3 wells were used.

For the colony formation assay, UC9 and EJ cells were transfected with expression vector or siRNAs. Trypsin-treated cells were suspended in medium containing DMEM or RPMI-1640 medium with 10% FBS, antibiotics, and 3 mL of 0.35% noble agar (Difco). Cells (1×10^5 cells/well) were plated onto a solidified medium containing 3 mL of 0.7% noble agar in a 60-mm dish. The dishes were incubated at 37°C with 5% CO_2, and fresh medium was added every 4 to 5 days. UC9 were grown for 35 days, and EJ were incubated for 21 days before staining with 0.05% crystal violet. We counted forming colonies (>100 μm in diameter) using microscopy.

Invasion and migration assays and tumor xenograft assay

For cell invasion assays, we used a Boyden chamber (NeuroProbe) and membrane (8-μm pore size) precoated with growth factor–reduced Matrigel (BD Biosciences). After 24 hours of transfection, bladder cancer cells in 56 μL of medium without FBS were seeded (5×10^4 cell/well) in the upper chamber. In the lower chamber, 27 μL of medium with 0.1% FBS medium (5637, EJ) and 10% FBS medium (UC5, UC9) was added as a chemoattractant. Then, cells were incubated for 12 hours (5637, EJ) and 24 hours (UC5, UC9).

For cell migration assays, the procedure was similar to the cell invasion assay, except Transwell membranes precoated with collagen (Sigma-Aldrich) were used, and cells were incubated for 12 hours (5637, EJ) and 24 hours (UC5, UC9). After staining the membrane using Diff-Quik reagents (Sysmex Co.), cells adhering to the lower surface were counted using a light microscope at 50× and 200× magnification and at least 4 wells were selected for each experimental group.

For the tumor xenograft assay, 4-week-old male BALB/c nude mice were obtained from SLC (Japan SLC, Inc.) and maintained under pathogen-free conditions. Knockdown- or overexpressed cells (KD-EJ, 1×10^6 cells; UC9, 2×10^6 cells) were suspended in 100 μL PBS. Cells were injected subcutaneously into both flanks on the top and bottom of mice. Tumor diameters were measured every 3 days for 3 weeks postinjection using digital calipers. Tumor volume in cubic millimeters was calculated using the formula: $(L \times W^2) \times 0.52$, where L is the maximum length and W is the maximum width.

Chromatin immunoprecipitation assay

Chromatin immunoprecipitation (ChIP) assay was carried out as previously described (22) with primer sets (in Supplementary Methods S2) for *EZH2* and *SUZ12* promoter used for the qPCR.

Chemoresistance assay

Cells were seeded at a density of 1×10^5 cells per well, and transfection of plasmids was carried out using the jetPRIME reagent (Polyplus Transfection Inc.) according to the manufacturer's protocol for 12 hours. After transfection, the medium was changed with 0 or 5 μmol/L of mitomycin C (MMC, Sigma) and 10 μmol/L of cisplatin (Dong-A ST) for 12 hours.

Results

Biologic insights into the gene expression signature associated with disease progression

Using gene expression data of 102 NMIBCs in the Korean cohort (GSE13507; ref. 8), we selected *in trans* genes correlated with the *E2F1* (total 1441 genes by the Pearson correlation test, $P < 0.001$, $r > |0.4|$). Gene-to-gene network and upstream regulator analyses were performed using IPA tool displayed several important regulators with their effectors (i.e., gene networks) associated with disease progression of NMIBC (Supplementary Table S1). The path-exploring function of IPA revealed that an interconnection of network hubs composed of *E2F1*, *EZH2*, and *SUZ12* is involved in a signaling pathway strongly associated with NMIBC progression (Fig. 1A). The patients in the Korean cohort were separated into the EH (E2F1 high expression) subgroup and the EL (E2F1 low expression) subgroup (two-sample t test, $P < 0.001$; Fig. 1B), indicating that activation of *E2F1*, the most predominant regulator,

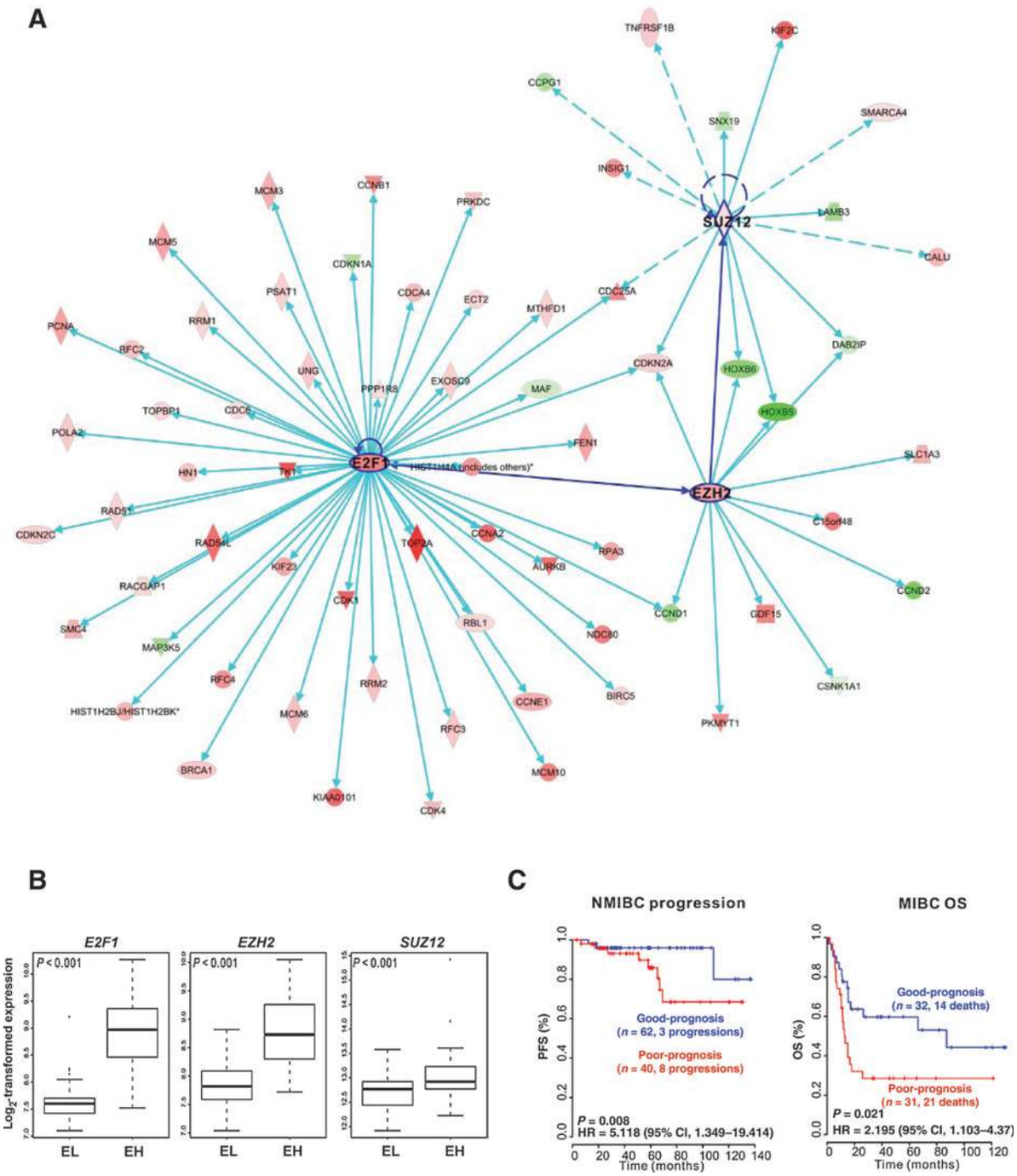

Figure 1.

Association between gene signature and PFS of NMIBC in the Korean cohort ($n = 102$). A, a predominant signaling pathway consisting of *E2F1*, *EZH2*, and *SUZ12* associated with disease progression of NMIBC. Up- and downregulated genes in the EH group are indicated in red and green, respectively. The intensity of color is indicative of the degree of over- or underexpression. Each line and arrow represents functional and physical interactions between the genes and the direction of regulation reported in the literature. B, two-group boxplot comparing expression levels of *E2F1*, *EZH2*, and *SUZ12* in EH (a high *E2F1* cluster) and EL (a low *E2F1* cluster) patients. Each *P* value was obtained by two-sample *t* test between EH and EL. C, survival estimation, NMIBC progression, MIBC OS, with a signature composed of 3 genes, *E2F1*, *EZH2*, and *SUZ12*.

might be a key event associated with the progression of NMIBC. *E2F1* was interconnected with another gene network hub composed around *EZH2* that was interconnected with *SUZ12* network (Fig. 1A). *EZH2* was more highly expressed in the EH subgroup than in the EL subgroup (two-sample *t* test, $P < 0.001$; Fig. 1B). The expression of *SUZ12* was also significantly

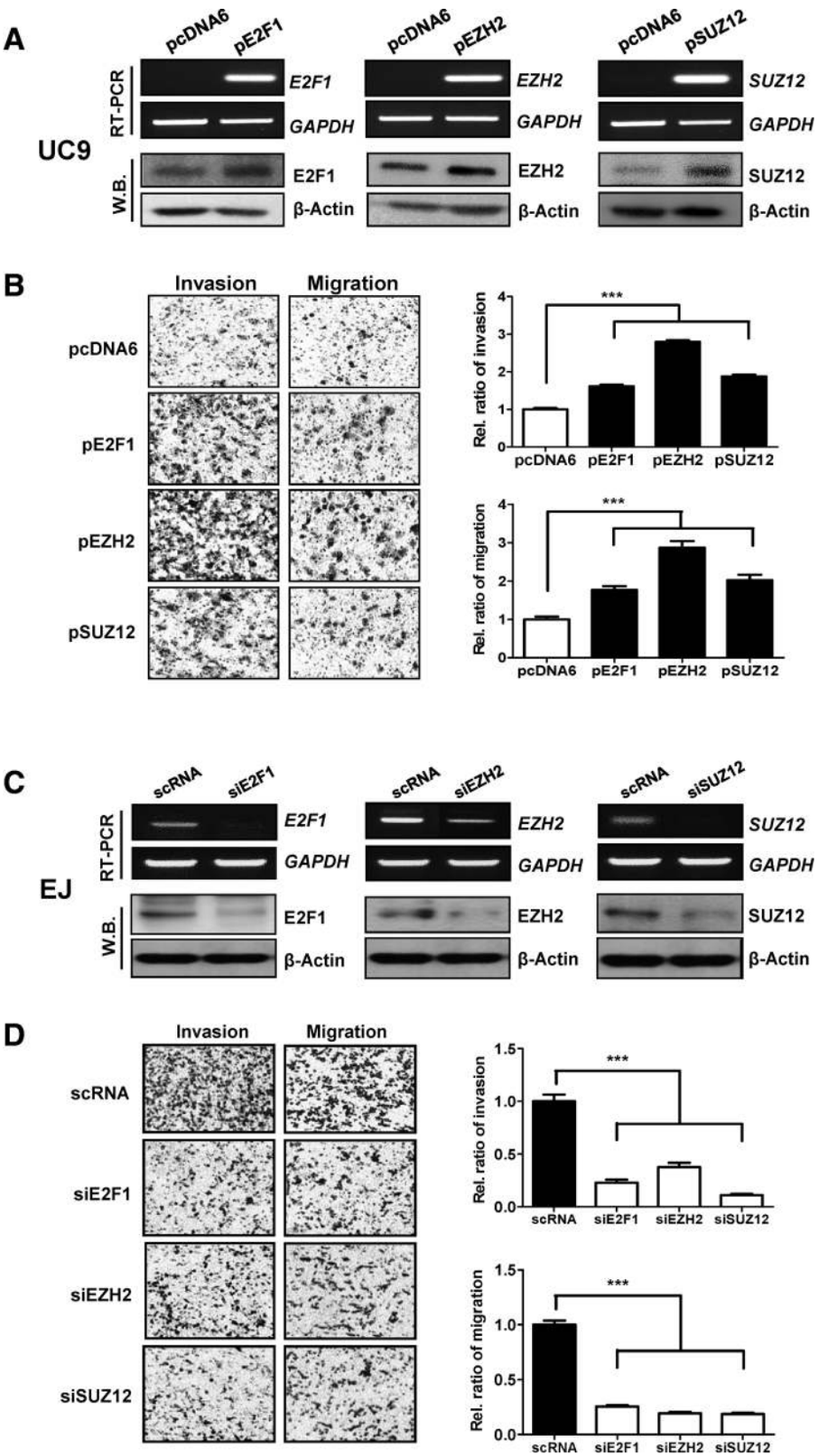

Figure 2.
Alternative expression of *E2F1*, *EZH2*, and *SUZ12* regulates invasion and migration in bladder cancer. A and B, effects of overexpression of *E2F1*, *EZH2*, and *SUZ12* genes in UC9 cells. A, cells overexpressing pE2F1, pEZH2, or pSUZ12 compared with cells with control vector (pcDNA6). Upregulation of mRNA and protein expression were detected by RT-PCR and Western blotting. B, cell overexpressing *E2F1*, *EZH2*, and *SUZ12* showed increased cell migration and invasion. C and D, effects of knockdown (KD) of *E2F1*, *EZH2*, and *SUZ12* genes in EJ cells. C, downregulation of mRNA and protein expression was detected in cells with siE2F1, siEZH2, or siSUZ12 compared with cells with control (scRNA). Downregulated *E2F1*, *EZH2*, and *SUZ12* cells showed reduced invasion and migration. Data are presented as mean ± SD for 3 independent experiments (original magnification, 200×). ***, $P < 0.001$.

higher in the EH subgroup than in the EL subgroup (two-sample t test, $P < 0.001$; Fig. 1B).

The PFS analysis in NMIBCs ($n = 102$) using a signature combined with *E2F1*, *EZH2*, and *SUZ12* (the 3-gene signature) showed a significant difference of progression rates in NMIBC between poor- and good-prognosis subgroups ($P = 0.008$; Fig. 1C, left). To validate a prognostic value of the signature of 3 genes in NMIBC progression, we tested the signature in independent patient cohorts (GSE32894, GSE32548, and GSE19915). Because all validation cohorts did not contain PFS time data, we alternatively validated the signature by receiver operating characteristic (ROC) analysis comparing PI scores and NMIBC progression events. High or moderate area under curve (AUC) values were observed in all 3 patient cohorts (AUCs = 0.71, 0.59, and 0.65 in GSE32894, GSE32548, and GSE19915, respectively; Supplementary Fig. S1), indicating that the 3-gene signature would be highly associated with NMIBC progression. Using PI scores, patients were divided into 2 groups (poor- or good-prognosis), in which proportions of disease progression were also assessed. Significant differences of progression between poor and good prognosis groups were obtained from the datasets except for GSE32548 (Fisher exact test: $P < 0.001$, $P = 0.459$, and $P = 0.049$ in GSE32894, GSE32548, and GSE19915, respectively). However, the ratios of disease progression in the poor-prognosis group

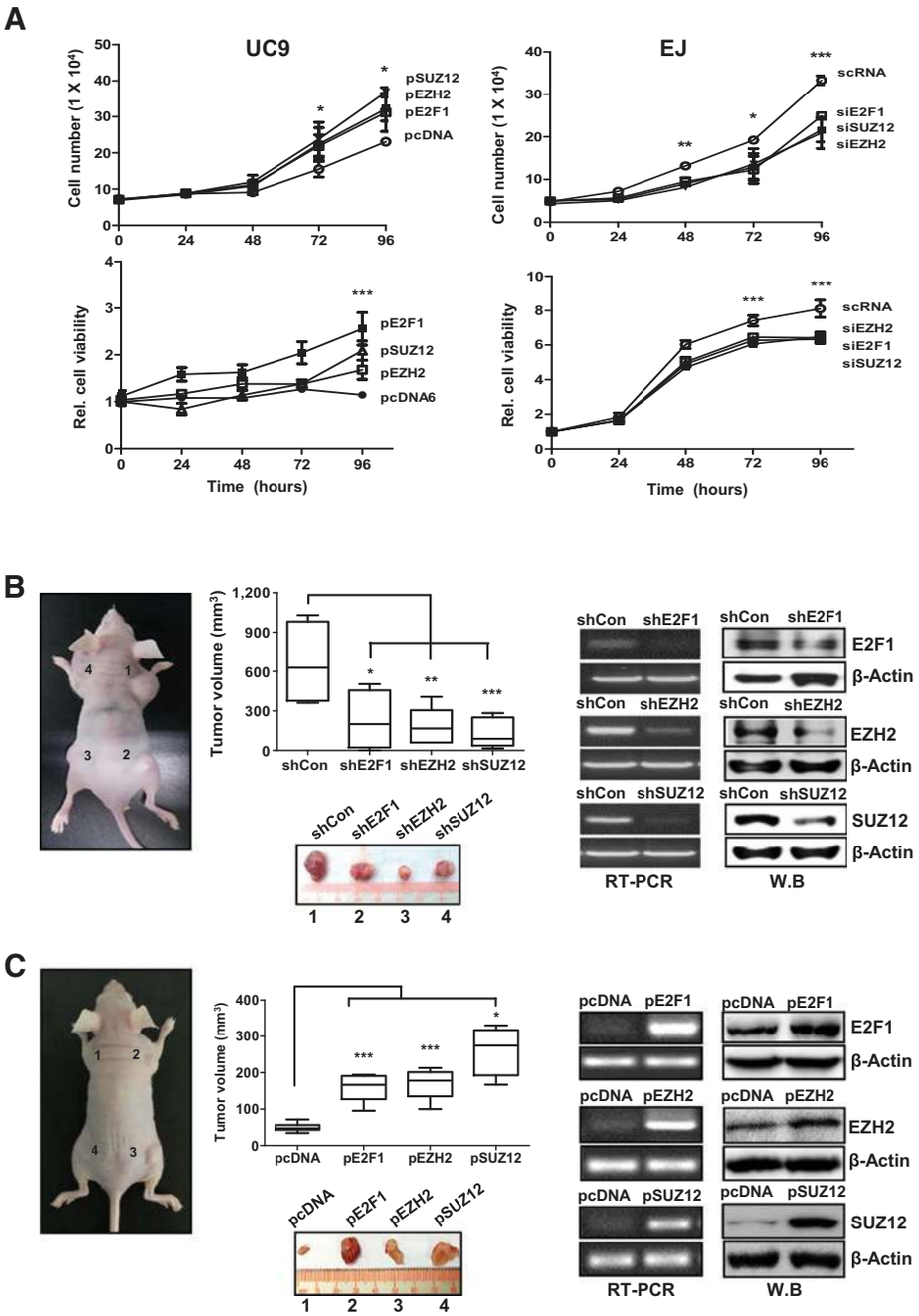

Figure 3.
Effect of alternative expression of *E2F1*, *EZH2*, and *SUZ12* on cell proliferation and tumorigenesis. A, UC9 cells overexpressing *E2F1*, *EZH2*, or *SUZ12* showed significantly higher cell proliferation and cell viability than that of empty vector–transfected cells (pcDNA6; left). The siE2F1, siEZH2, or siSUZ12-KD EJ cells showed decreased cell proliferation and cell viability (right). B, tumor volume from xenografted nude mice with control shRNA, shE2F1, shEZH2, or shSUZ12 cell lines. Injection of shE2F1, shEZH2, or shSUZ12 cell lines showed a significant decrease in tumor growth compared with control-treated groups. Volumes of tumors dissected from the sacrificed mice (*, $P < 0.01$). The decreased RNA and protein levels from the resected tumors are represented in right. C, tumor volume from xenografted nude mice with transfected UC5 cells with control pCDNA, pE2F1, pEZH2, or pSUZ12 overexpression vector. Injection of transfected pE2F1, pEZH2, or pSUZ12 cell lines showed a significant increase in tumor growth compared with control pCDNA groups. Volumes of tumors dissected from the sacrificed mice (*, $P < 0.01$). The increased RNA and protein levels from the resected tumors are represented in right.

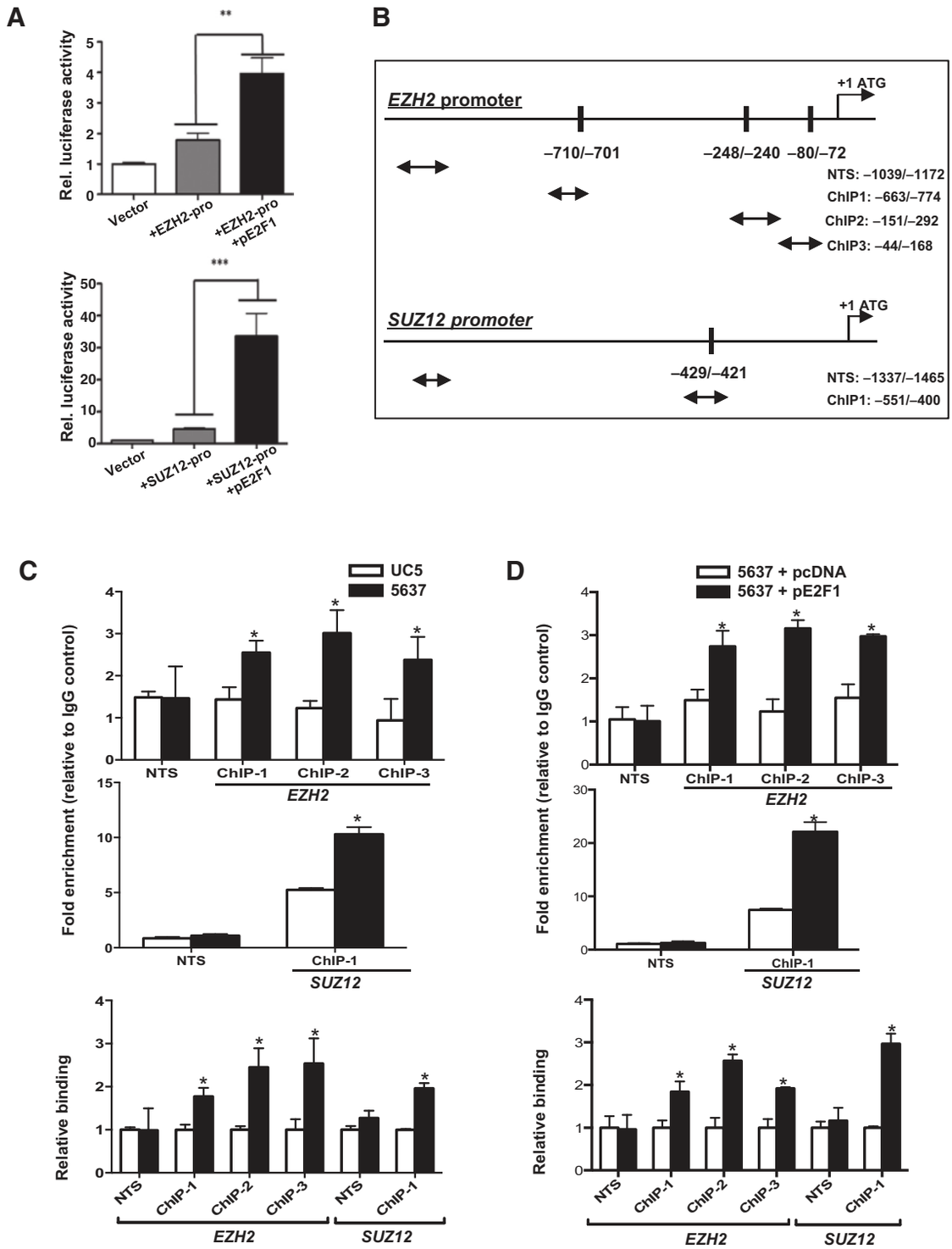

Figure 4.

E2F1 regulates the expression of *EZH2* and *SUZ12* by directly binding to their promoter region. A, the E2F1-binding site on the promoter region of *EZH2* or *SUZ12* was confirmed by luciferase assay in 5637 cells after cotransfection with pE2F1 and a plasmid (EZH2-pro or SUZ12-pro) containing a fragment of the promoter region of *EZH2* or *SUZ12*. B, putative binding sites for E2F1 were found in the promoter regions of *EZH2* (−710/−701, −248/−240, and −80/−72) and one site in *SUZ12* (−429/421). ChIP-qPCR analyses were performed in untreated UC5 and 5637 cells (C), whereas it was examined in 5637 cells with transfected pcDNA or pE2F1 (D) using the E2F1 antibody. C, the top 2 represent fold enrichment with E2F1 antibody compared with IgG in the promoter regions of *EZH2* and *SUZ12* versus NTS region in untreated UC5 and 5637 cells, and the bottom shows the relative binding in 5637 cells compared with UC5 cells. D, the top 2 represent fold enrichment with E2F1 antibody compared with IgG with the pcDNA or pE2F1 activities in 5637 cells, and the bottom shows the relative binding in the pE2F1 activities versus pcDNA controls. Data represent the mean ± SE of 3 independent experiments. *, $P < 0.05$ (*t* test).

(21.3%, 12.2%, and 22.2%) were still higher than in the good-prognosis group (5%, 5.8%, and 7%) in all 3 validation cohorts (GSE32894, GSE32548, and GSE19915), respectively (Supplementary Fig. S1). In addition to NMIBC progression, we also assessed OS of MIBC using the 3-gene signature. The OS of MIBC ($n = 63$) in the poor-prognosis subgroup was also significantly worse than that in the good-prognosis subgroup ($P = 0.021$; Fig. 1C, right). For validation in OS of MIBC, we tested the signature in an independent combined cohort with GSE32984 and GSE32548, in which the survival rate of MIBC in the poor-prognosis subgroup classified by the signature of 3 genes was significantly worse than that in the good-prognosis subgroup ($P = 0.044$; Supplementary Fig. S2A).

To provide comparative results with other signatures, we additionally illustrated Supplementary Fig. S2 and described a comparative analysis between the signatures in "Comparison of other signatures with the three-gene signature" subsection in Supplementary Text S1. Because a previously published signature for predicting progression of NMIBC (23) consisted of small number of genes (the 11-gene signature) like our signature, we tried to compare them (Supplementary text S1). As shown in Supplementary Text and Supplementary Fig. S2, the 3-gene signature is validated a significant prognostic value.

Characterization of bladder cancer cell lines by unsupervised hierarchical clustering analysis and functional study

We tested the characteristics of various bladder cancer cell lines that were derived from diverse stages of bladder cancer tissues. Unsupervised hierarchical clustering analysis of gene expression data from 19 bladder cancer cell lines yielded 3 major clusters, one representing the more aggressive (MIBC-like) and the other less aggressive (NMIBC-like) cancer cells (Supplementary Fig. S3A). These gene expression patterns may reflect the molecular configurations that are readily distinguishable between more aggressive (MIBC-like) and less aggressive (NMIBC-like) cancer cells.

To determine the microarray data that divided cases into NMIBC and MIBC subgroups, the biologic characteristics of total 12 bladder cancer cell lines were assessed by their invasiveness (Supplementary Fig. S3B). UC5, UC9, UC1, and UC6 cell lines showed characteristics of NMIBC, whereas others (UC3, UC10, UC14, 5637, EJ, T24, KU7, J82) were similar to MIBC (Supplementary Fig. S3B). Thus, we selected 4 cell lines as representative members in 2 characterized subgroups (NMIBC and MIBC) for further studies; UC5 and UC9 were NMIBC and EJ and 5637 were MIBC cells. The expression levels of *E2F1*, *EZH2*, and *SUZ12* in the 2 groups of bladder cancer cells were evaluated by quantitative RT-PCR and Western blot assay. The mRNA expression of *E2F1*, *EZH2*, and *SUZ12* in NMIBC was significantly lower than in MIBC cells ($P < 0.01$; Supplementary Fig. S3C). Protein levels of these genes were also increased in MIBC cells compared with NMIBC cells (Supplementary Fig. S3D). Thus, higher expression of these genes is clearly preserved in invasive cancer cells (Supplementary Fig. S3C and S3D), indicating possible mechanisms that contribute to progression to invasive or metastatic bladder tumors.

The *E2F1–EZH2–SUZ12* signature is strongly associated with the progression of noninvasive tumors to invasive tumors

To determine whether the *E2F1–EZH2–SUZ12* signature mediates progression from NMIBC to MIBC, we performed a number of *in vitro* and *in vivo* assays. As previously described, we examined the endogenous expression levels of *E2F1*, *EZH2*, and *SUZ12* and compared them between NMIBC and MIBC (Supplementary Fig. S3C and S3D). Expression changes in the overexpressed cells with *E2F1*, *EZH2*, and *SUZ12* may reflect cancer cell invasion and/or migration properties if these genes are strongly related to tumor progression. Comparisons of the expression levels of these genes between UC9 cells transfected with the pcDNA6 control vector and with pE2F1, pEZH2, or pSUZ12 are shown in Fig. 2A. Cells overexpressing *E2F1*, *EZH2*, and *SUZ12* showed significant increases in both invasion and migration (Fig. 2B). In addition, in NMIBC UC5 cells, the effects of increasing the expression of *E2F1*, *EZH2*, and *SUZ12* were also examined (Supplementary Fig. S4).

We also investigated the effects of silencing *E2F1*, *EZH2*, and *SUZ12* expression using siRNA in EJ (Fig. 2C). EJ cells with decreased *E2F1*, *EZH2*, and *SUZ12* expression displayed a significant decrease in invasiveness and migration (Fig. 2D). These results demonstrate that the increased expression of *E2F1*, *EZH2*, and *SUZ12* is related to the invasiveness and migratory characters of bladder cancer cells. In addition, MIBC-5637 was also examined to confirm the effect of silencing of *E2F1*, *EZH2*, and *SUZ12* (Supplementary Fig. S5).

Redundant role of elevated *E2F1*, *EZH2*, and *SUZ12* in proliferation, viability, and tumorigenesis of NMIBC cells

To investigate whether the *E2F1*, *EZH2*, and *SUZ12* affect cell proliferation and viability of NMIBC cells, cell proliferation was evaluated by counting the number of cells every day. As shown in Fig. 3A, top (left), *E2F1*-, *EZH2*-, or *SUZ12*-overexpressing UC9 significantly promoted cell proliferation compared with pcDNA. Otherwise, the depletion of these genes by siRNAs suppressed proliferation of EJ cancer cells (Fig. 3A, top right). We also found that the viability of cells overexpressing these genes was significantly higher than in the control group at 96 hours (Fig. 3A, bottom). In contrast, depletion of these genes by siRNA suppressed the viability of EJ cancer cells, compared with siControl-transfected cells at 72 and 96 hours (Fig. 3A, bottom right). These results suggest that elevated these genes may be related to bladder cancer cell proliferation and viability.

To obtain *in vivo* insight for these observations, nude mice were inoculated with E2F1-KD, EZH2-KD, or SUZ12-KD cell lines. The decreased mRNA and protein levels of shE2F1, shEZH2, or shSUZ12 cells are shown in Supplementary Fig. S6. All mice inoculated with shE2F1, shEZH2, or shSUZ12 cell lines showed a significant decrease in tumor volume compared with control-treated groups (Fig. 3B). Decreased expression levels of E2F1, EZH2, or SUZ12 from the resected tumors were also detected (Fig. 3B, right).

To examine the redundant role of elevated *E2F1–EZH2–SUZ12* in proliferation and tumorigenesis in NMIBC cells, we also performed the reverse (overexpression) model in a tumor xenograft assay (Fig. 3C). All mice inoculated with overexpressed elevated *E2F1–EZH2–SUZ12* cells showed a significant increase in tumor volume compared with control (pcDNA6) groups (Fig. 3C). Increased mRNA and protein levels from the resected tumors were also represented (Fig. 3C, right).

The alternative expressions of *EZH2* and *SUZ12* are regulated by *E2F1* in bladder cancer cells

To identify whether E2F1 directly regulates transcription of the *EZH2* and *SUZ12* genes, we used the *EZH2* and *SUZ12* promoter

vectors to drive a luciferase reporter gene in transient cotransfections with an *E2F1* expression plasmid in 5637. Ectopic *E2F1* strongly upregulated transcription from the both promoters in the 5637 (Fig. 4A). To determine the *in vivo* interaction of E2F1 with 3 potential E2F1-binding sites in the *EZH2* promoter region or 1 potential E2F1-binding site in the *SUZ12* promoter region (Fig. 4B), ChIP assays were performed using an E2F1 antibody. The appropriate *EZH2* and *SUZ12* promoter regions were immunoprecipitated with the E2F1 antibody (Fig. 4C and D). ChIP-qPCR analyses revealed that PCR fragments containing the potential *E2F1*-binding site at 3 regions in the *EZH2* promoter and 1 region in the *SUZ12* promoter were markedly increased in DNA samples from *E2F1*-transfected cells compared with DNA from pcDNA-transfected cells (Fig. 4C and D). No detectable band was observed in the control IgG precipitations.

To further define the mechanistic link between *E2F1* and *EZH2* or *SUZ12*, we tested whether expression levels of *EZH2* or *SUZ12* showed a transient change in *E2F1*-overexpressing UC9 (pE2F1, Fig. 5A, left) and in siE2F1-treated EJ (siE2F1, Fig. 5A, right). These experiments demonstrated that the overexpression of *E2F1* activity induced *EZH2* and *SUZ12* expression, and the loss of *E2F1* activity reduced *EZH2* and *SUZ12* expression (Fig. 5A). Consistent with the ChIP assays, these results suggest that E2F1 directly regulates transcription of the *EZH2* and *SUZ12*.

To assess whether the lack of *E2F1* is complemented by *EZH2* or *SUZ12* in cancer progression, we independently overexpressed the *EZH2* or *SUZ12* in E2F1-KD cells. In both E2F1-KD cells (shE2F1#1 and shE2F1#2), mRNA expression of *EZH2* or *SUZ12* was reduced compared with controls (shCon), whereas it was effectively restored by *EZH2* or *SUZ12* overexpression (Fig. 5B). Then, to verify whether the invasion ability of *E2F1* was also rescued by *EZH2* or *SUZ12*, we determined the level of invasion of E2F1-KD cells and cells overexpressing *EZH2* or *SUZ12* in E2F1-KD cells. E2F1-KD decreased invasion ability, which was significantly restored by *EZH2* or *SUZ12* overexpression (Fig. 5C and D).

Elevated *E2F1*, *EZH2*, and *SUZ12* expression is related to sphere formation and chemoresistance in bladder cancer cells

Recent investigations demonstrated that tumorigenicity and tumor progression are driven by CSC characteristics, and the expression of *EZH2* was consistently upregulated in CSCs (24–26). It also has been reported that *SUZ12* is important for the function of CSCs, and ectopic expression of *SUZ12* in transformed cells is sufficient to generate CSCs (27, 28). To elucidate the relationship between the *E2F1–EZH2–SUZ12* signature and the CSC characteristics, we analyzed the ability of sphere formation and chemoresistance in bladder cancer cells.

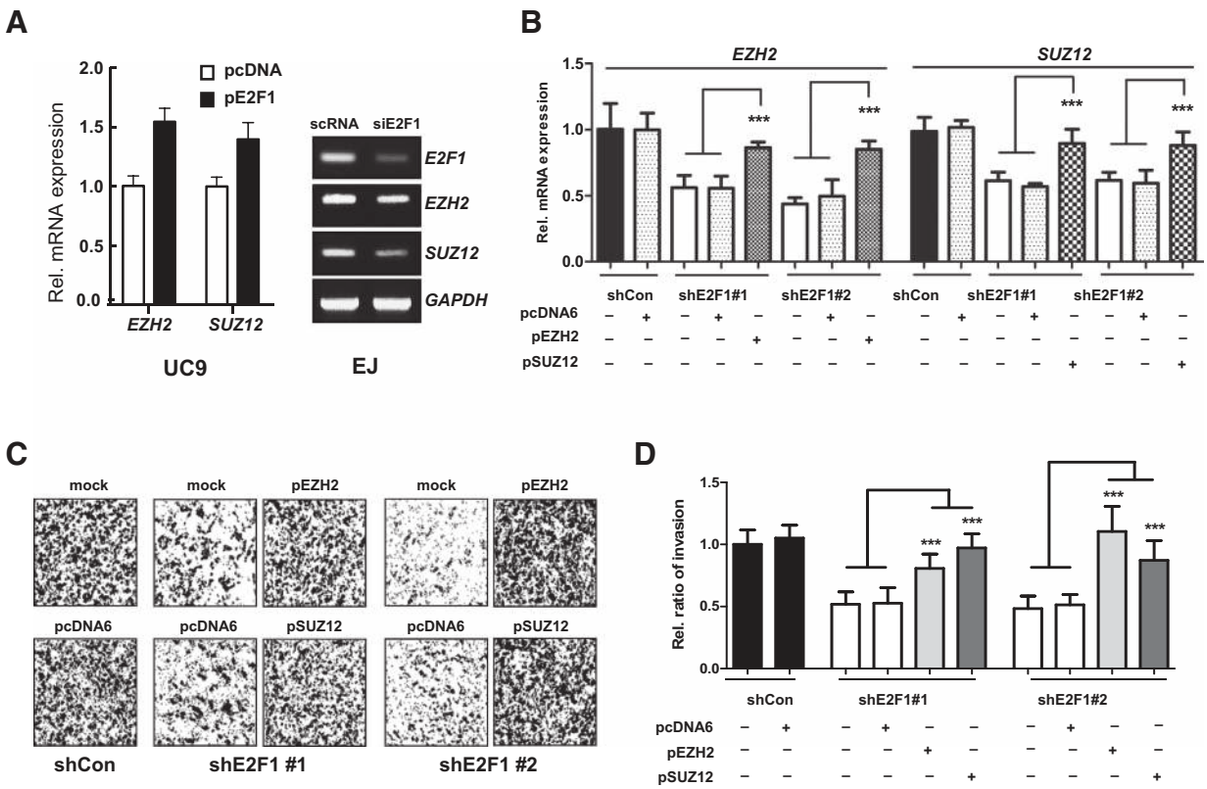

Figure 5.
E2F1 controls expression of *EZH2* and *SUZ12* in bladder cancer cells. A, *E2F1* KD decreases the expression of *EZH2* and *SUZ12* in bladder cancer cells. Left, UC9 cells show upregulation of *EZH2* and *SUZ12* by *E2F1* overexpression. Right, EJ cells show underexpressed *EZH2* and *SUZ12* expression with *E2F1*-targeted siRNA (siE2F1) compared with scrambled control (scRNA). B, *E2F1* KD (shE2F1) leads to downregulation of *EZH2* and *SUZ12* when compared with controls (shCon). Downregulation was suppressed by pcDNA6-*EZH2* or -*SUZ12* overexpression vectors, but not by pcDNA empty vector. C, representative images of entire invaded and stained chambers are shown. Decreased invasion of EJ cells with *E2F1*-targeted shRNA (shE2F1#1, #2) compared with scrambled shRNA (NTS). Reduced invasive ability was effectively suppressed by *EZH2* (+pEZH2) or *SUZ12* (+pSUZ12) overexpression but not by pcDNA empty vector. D, results shown on the graph represent means ± SD of 3 independent experiments. *, $P < 0.05$; **, $P < 0.01$; ***, $P < 0.001$.

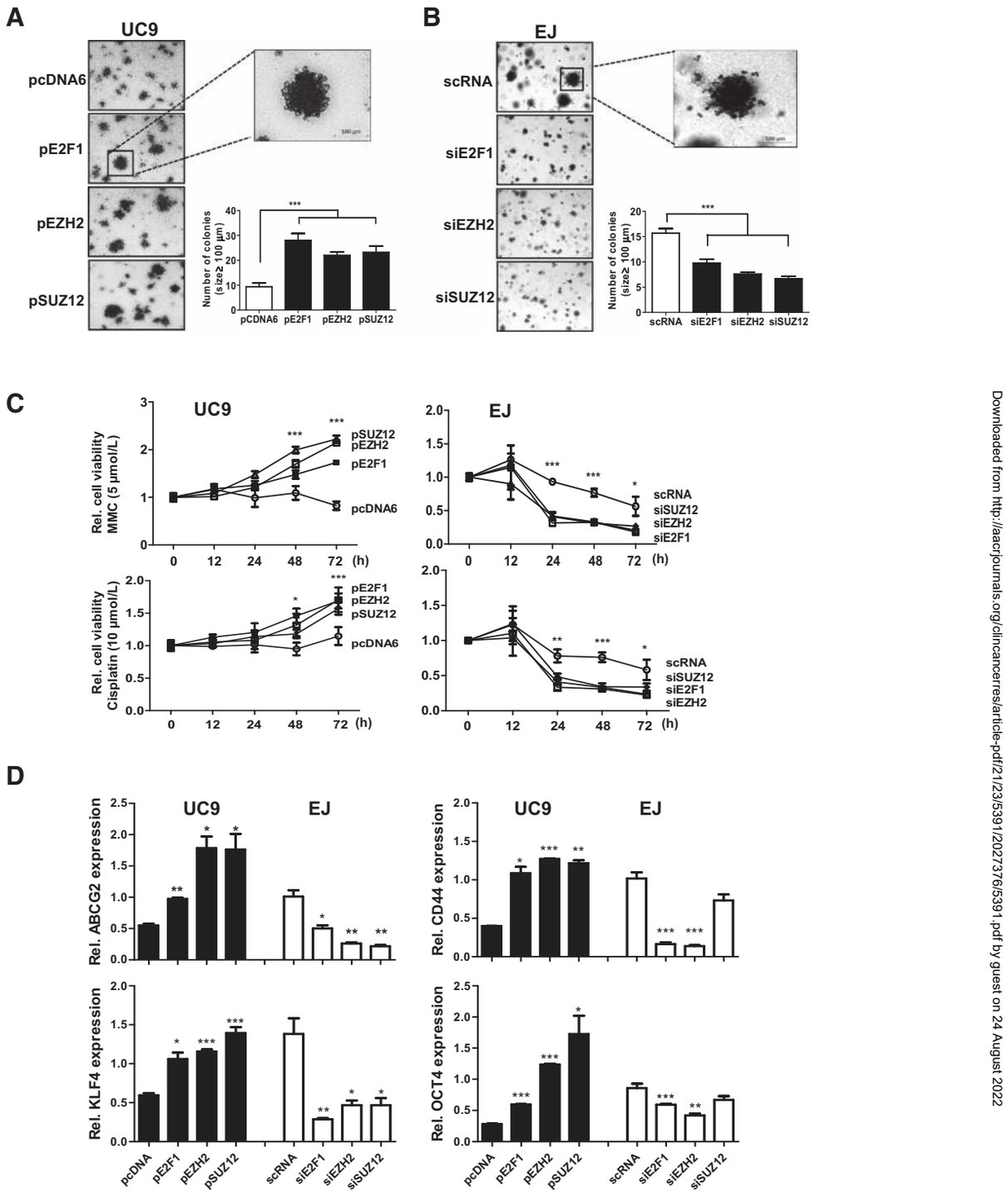

Figure 6.

Colony formation ability and CSC signatures were compared between cells with alternative expressed *E2F1*, *EZH2*, or *SUZ12* vector and control cells. A, representative images of colony formation of UC9 bladder cancer cells transfected with pcDNA6-V5-His-empty vector and pcDNA6-V5-His-*E2F1*, -*EZH2*, or -*SUZ12* overexpression vectors. Quantitative analysis of colony numbers is shown as a graph that counted colonies larger than 100 μm in diameter. B, the number of colonies was reduced in EJ cells treated with si*E2F1*, si*EZH2*, or si*SUZ12* compared with cells treated with siControl. C, UC9 transfected with pcDNA, pE2F1, pEZH2, or pSUZ12 and EJ treated with siE2F1, siEZH2, or siSUZ12 were treated with MMC (5 μmol/L, top) and cisplatin (10 μmol/L, bottom). UC9 cells transfected with pE2F1, pEZH2, or pSUZ12 showed significantly higher cell viability than that of empty vector–transfected cells (pcDNA) by the MTT assay. Controversially, EJ cells treated with siRNA represented significantly lower cell viability than control (scRNA). ○, pcDNA or scRNA; ●, pE2F1 or siE2F1; Δ, pEZH2 or siEZH2; ■, pSUZ12, siSUZ12. D, CSC signatures were analyzed under anticancer drug-treated conditions. UC9 cells (transfected with pcDNA, pE2F1, pEZH2, or pSUZ12) and EJ cells (treated with scRNA, siE2F1, siEZH2, and siSUZ12) were treated with 5 μmol/L MMC. Values are the mRNA expression levels in MMC-treated cells relative to untreated cells. Results shown on the graph represent means ± SD of 3 independent experiments. *, $P < 0.05$; **, $P < 0.01$; ***, $P < 0.001$.

Colony-forming assay was performed to verify whether the elevated expression of *E2F1*, *EZH2*, or *SUZ12* is critical for sphere formation. Overexpression of *E2F1*, *EZH2*, or *SUZ12* in UC9 significantly increased the number of large colony (>100 μm of diameter) formation compared with control (pcDNA6-empty; Fig. 6A, top). Otherwise, the depletion of *E2F1*, *EZH2*, or *SUZ12* in the invasive EJ cells by each siRNAs for *E2F1*, *EZH2*, or *SUZ12* decreased the number of large colony formation compared with control treated with scRNA (Fig. 6B).

To determine the chemoresistance which is known as one of CSC characteristics, the cell viability of *E2F1*-, *EZH2*-, or *SUZ12*-overexpressing cells was determined after the treatment of 5 μmol/L MMC (Fig. 6C, top) and 10 μmol/L cisplatin (Fig. 6C, bottom). Overexpression of *E2F1*, *EZH2*, or *SUZ12* in UC9 and UC5 significantly increased the viability compared with control, whereas the depletion of *E2F1*, *EZH2*, or *SUZ12* in the invasive EJ cells by each siRNAs decreased viability compared with control (Fig. 6C and Supplementary Fig. S8). Furthermore, mRNA levels of *CD44*, *KLF4*, *OCT4*, and *ABCG2* known as CSC markers (29–32) significantly affected in under MMC- or cisplatin-treated conditions in bladder cancer cells with altered *E2F1*, *EZH2*, and *SUZ12* expression than in matched control group (Fig. 6D and Supplementary Fig. S7).

Discussion

According to the success of recent genome-wide gene expression profile studies (33–35), we previously reported a prognostic signature for predicting the progression of superficial tumors to invasive ones (8). The higher biologic activity of E2F1 suggests that it may be the major driving force during the progression of bladder cancer. Gene network analyses of the signature revealed that *E2F1* and its downstream effectors *EZH2* and *SUZ12* could be important mediators for the invasive and metastatic progression of superficial tumors (Fig. 1). Consistent with other cancers, the relationship between cancer progression and the overexpression of these genes was observed (36–41). Recently, Santos and colleagues (42) also reported that the increased tumor recurrence and progression in patients with NMIBC is associated with increased E2F and *EZH2* expression.

Overexpression of *EZH2* and *SUZ12* is directly controlled by *E2F1* (Fig. 4), and their expression is associated with poor prognosis and indicative of invasion and metastasis in many cancers (Figs. 2 and 3). Our results show that these prognostic molecules can predict the likelihood of progression of NMIBC. Furthermore, unequal distribution of expression patterns reflecting activation of *E2F1* in subgroups (EL, EH) with different progression rates supports the notion that distinct molecular features of the tumor govern the clinical phenotypes of NMIBC. As a result, we speculate that the overexpression of *E2F1–EZH2–SUZ12* may play a role in proliferation, migration, and invasion of cancer cells.

It has been known that CSC characteristics may lead to cancer aggressiveness, chemoresistance to anticancer drugs, and a high risk of recurrence in patients with cancer (29, 31, 32, 43). Recent reports suggest that tumorigenicity and tumor progression is driven by CSC characteristics, and CSCs consistently showed elevated *EZH2* and *SUZ12* expression (24–28). It also has been reported that *EZH2* and *SUZ12* is important for the function of CSCs and its ectopic expression in transformed cells is sufficient to generate CSCs (24–28). Thus, we investigated the association of the *E2F1–EZH2–SUZ12* downstream targets with the characteristics of CSCs. To identify the characteristics of CSCs, the abilities of sphere formation and chemoresistance were determined. The capacity of sphere formation is determined by both the proliferation rate and cell adhesion ability and has been used to identify the characteristic of CSCs in the previous studies (44–46). In this study, overexpression of *E2F1–EZH2–SUZ12* increased the formation of large sphere, and the depletion of these genes decreased the formation of large sphere, which suggest that these genes might play important roles in sphere formation. Also, an increase in viability of the *E2F1–EZH2–SUZ12*–overexpressing cells under the treatment of MMC or cisplatin reflects that *E2F1*, *EZH2*, *or SUZ12* might be related with resistance of the cells to anticancer drug. In addition, the activation of stem cell–like molecules (*CD44*, *OCT4*, *KLF4*, and *ABCG2*) was detected in bladder cancer cells overexpressing *E2F1*, *EZH2*, and *SUZ12*. Moreover, the activation of *ABCG2* and *CD44* could be related to the chemoresistance of the cells and, consequently, enriching CSCs by drug treatment might induce cancer aggressiveness (30, 47, 48).

We would suggest that the activation of *EZH2* and *SUZ12* expression under the control of *E2F1* might play a role of switch in the development of bladder cancer according to tumor microenvironment. If the tumor microenvironment is favorable for cancer growth, the overexpression of *EZH2–SUZ12* signature by *E2F1* regulation contributes to the proliferation and invasiveness of bladder cancer cells. However, under the condition of anticancer drug treatment, the *EZH2–SUZ12* signature by *E2F1* control might activate CSCs signatures. As results, overexpressed *E2F1–EZH2–SUZ12* cells have significantly higher capacities for sphere formation and activate the stem cell–like molecules when cells were put on an anticancer drug-treated condition.

Taken together, the elevated *E2F1–EZH2–SUZ12* expression in bladder cancer cells might play important roles in proliferation, migration, and invasiveness. Moreover, the enrichment of cells with the characteristics of CSCs by overexpression of these genes might play critical roles in chemoresistance and tumorigenicity, which might be associated with poor prognosis of bladder cancer cells. Therefore, our findings show that a prognostic molecular signature, *E2F1–EZH2–SUZ12*, can predict the likelihood of progression of NMIBC. Furthermore, our study could provide useful information to predict an individual's risk of progression and to establish a suitable chemotreatment for disease.

Disclosure of Potential Conflicts of Interest

No potential conflicts of interest were disclosed.

Authors' Contributions

Conception and design: J. Heo, I.-S. Chu, S.-H. Leem
Development of methodology: H.-H. Lee, I.-S. Chu
Acquisition of data (provided animals, acquired and managed patients, provided facilities, etc.): S.-R. Lee, Y.-G. Roh, S.-K. Kim, J.-S. Lee, S.-Y. Seol, H.-H. Lee, W.-T. Kim, I.-S. Chu
Analysis and interpretation of data (e.g., statistical analysis, biostatistics, computational analysis): S.-K. Kim, J.-S. Lee, J. Heo, T.-H. Kang, I.-S. Chu, S.-H. Leem
Writing, review, and/or revision of the manuscript: S.-R. Lee, Y.-G. Roh, S.-K. Kim, J. Heo, T.-H. Kang, I.-S. Chu, S.-H. Leem
Administrative, technical, or material support (i.e., reporting or organizing data, constructing databases): W.-J. Kim, H.-J. Cha, J.W. Chung, I.-S. Chu, S.-H. Leem
Study supervision: J. Heo, I.-S. Chu, S.-H. Leem

Grant Support

This research was supported by the Mid-Career Researcher Program through the National Research Foundation of Korea (NRF) grant (NRF-2013R1A2A2A04008115), an NRF grant (2008-0062611 and 2011-0019745) funded by the Korea government (MEST), and a grant from the KRIBB Research Initiative Program.

The costs of publication of this article were defrayed in part by the payment of page charges. This article must therefore be hereby marked *advertisement* in accordance with 18 U.S.C. Section 1734 solely to indicate this fact.

Received October 17, 2014; revised June 24, 2015; accepted July 28, 2015; published OnlineFirst August 12, 2015.

References

1. Siegel R, Naishadham D, Jemal A. Cancer statistics, 2013. CA Cancer J Clin 2013;63:11–30.
2. Youssef RF, Lotan Y. Predictors of outcome of non-muscle-invasive and muscle-invasive bladder cancer. ScientificWorldJournal 2011; 11:369–81.
3. Pow-Sang JM, Seigne JD. Contemporary management of superficial bladder cancer. Cancer Control 2000;7:335–9.
4. Messing EM. Urothelial tumors of the bladder. In:Wein AJ, Kavoussi LR, Novick AC, Partin AW, Peters CA, editor. Campbell-Walsh's urology. Philadelphia, PA: Saunders; 2007. p. 2417–30.
5. Herr HW. Tumour progression and survival in patients with T1G3 bladder tumours: 15-year outcome. Br J Urol 1997;80:762–5.
6. Holmang S, Hedelin H, Anderstrom C, Holmberg E, Busch C, Johansson SL. Recurrence and progression in low grade papillary urothelial tumors. J Urol 1999;162:702–7.
7. Vedder MM, Marquez M, de Bekker-Grob EW, Calle ML, Dyrskjot L, Kogevinas M, et al. Risk prediction scores for recurrence and progression of non-muscle invasive bladder cancer: an international validation in primary tumours. PloS One 2014;9:e96849.
8. Lee JS, Leem SH, Lee SY, Kim SC, Park ES, Kim SB, et al. Expression signature of E2F1 and its associated genes predict superficial to invasive progression of bladder tumors. J Clin Oncol 2010;28:2660–7.
9. van Leenders GJLH, Dukers D, Hessels D, van den Kieboom SWM, Hulsbergen CA, Witjes JA, et al. Polycomb-group oncogenes EZH2, BMI1, and RING1 are overexpressed in prostate cancer with adverse pathologic and clinical features. Eur Urol 2007;52:455–63.
10. Friedman JM, Liang GN, Liu CC, Wolff EM, Tsai YC, Ye W, et al. The putative tumor suppressor microRNA-101 modulates the cancer epigenome by repressing the polycomb group protein EZH2. Cancer Res 2009;69:2623–9.
11. Varambally S, Dhanasekaran SM, Zhou M, Barrette TR, Kumar-Sinha C, Sanda MG, et al. The polycomb group protein EZH2 is involved in progression of prostate cancer. Nature 2002;419:624–9.
12. Bachmann IM, Halvorsen OJ, Collett K, Stefansson IM, Straume O, Haukaas SA, et al. EZH2 expression is associated with high proliferation rate and aggressive tumor subgroups in cutaneous melanoma and cancers of the endometrium, prostate, and breast. J Clin Oncol 2006; 24:268–73.
13. Kleer CG, Cao Q, Varambally S, Shen R, Ota I, Tomlins SA, et al. EZH2 is a marker of aggressive breast cancer and promotes neoplastic transformation of breast epithelial cells. Proc Natl Acad Sci U S A 2003; 100:11606–11.
14. Chase A, Cross NC. Aberrations of EZH2 in cancer. Clin Cancer Res 2011;17:2613–8.
15. Herranz N, Pasini D, Diaz VM, Franci C, Gutierrez A, Dave N, et al. Polycomb complex 2 is required for E-cadherin repression by the Snail1 transcription factor. Mol Cell Biol 2008;28:4772–81.
16. Villa R, Pasini D, Gutierrez A, Morey L, Occhionorelli M, Vire E, et al. Role of the polycomb repressive complex 2 in acute promyelocytic leukemia. Cancer Cell 2007;11:513–25.
17. Sjodahl G, Lauss M, Lovgren K, Chebil G, Gudjonsson S, Veerla S, et al. A molecular taxonomy for urothelial carcinoma. Clin Cancer Res 2012; 18:3377–86.
18. Lindgren D, Sjodahl G, Lauss M, Staaf J, Chebil G, Lovgren K, et al. Integrated genomic and gene expression profiling identifies two major genomic circuits in urothelial carcinoma. PLoS One 2012;7: e38863.
19. Lindgren D, Frigyesi A, Gudjonsson S, Sjodahl G, Hallden C, Chebil G, et al. Combined gene expression and genomic profiling define two intrinsic molecular subtypes of urothelial carcinoma and gene signatures for molecular grading and outcome. Cancer Res 2010;70:3463–72.
20. Paik S, Shak S, Tang G, Kim C, Baker J, Cronin M, et al. A multigene assay to predict recurrence of tamoxifen-treated, node-negative breast cancer. N Engl J Med 2004;351:2817–26.
21. Kim SM, Leem SH, Chu IS, Park YY, Kim SC, Kim SB, et al. Sixty-five gene-based risk score classifier predicts overall survival in hepatocellular carcinoma. Hepatology 2012;55:1443–52.
22. Kim DH, Roh YG, Lee HH, Lee SY, Kim SI, Lee BJ, et al. The E2F1 Oncogene Transcriptionally Regulates NELL2 in Cancer Cells. DNA Cell Biol 2013; 32:517–23.
23. Catto JW, Abbod MF, Wild PJ, Linkens DA, Pilarsky C, Rehman I, et al. The application of artificial intelligence to microarray data: identification of a novel gene signature to identify bladder cancer progression. Eur Urol 2010;57:398–406.
24. Crea F, Hurt EM, Mathews LA, Cabarcas SM, Sun L, Marquez VE, et al. Pharmacologic disruption of Polycomb Repressive Complex 2 inhibits tumorigenicity and tumor progression in prostate cancer. Mol Cancer 2011;10:40.
25. Suva ML, Riggi N, Janiszewska M, Radovanovic I, Provero P, Stehle JC, et al. EZH2 is essential for glioblastoma cancer stem cell maintenance. Cancer Res 2009;69:9211–8.
26. Chang CJ, Yang JY, Xia W, Chen CT, Xie X, Chao CH, et al. EZH2 promotes expansion of breast tumor initiating cells through activation of RAF1-beta-catenin signaling. Cancer Cell 2011;19:86–100.
27. Iliopoulos D, Lindahl-Allen M, Polytarchou C, Hirsch HA, Tsichlis PN, Struhl K. Loss of miR-200 inhibition of Suz12 leads to polycomb-mediated repression required for the formation and maintenance of cancer stem cells. Mol Cell 2010;39:761–72.
28. Martin-Perez D, Sanchez E, Maestre L, Suela J, Vargiu P, Di Lisio L, et al. Deregulated expression of the polycomb-group protein SUZ12 target genes characterizes mantle cell lymphoma. Am J Pathol 2010;177:930–42.
29. Kumar SM, Liu S, Lu H, Zhang H, Zhang PJ, Gimotty PA, et al. Acquired cancer stem cell phenotypes through Oct4-mediated dedifferentiation. Oncogene 2012;31:4898–911.
30. Lu Y, Zhu H, Shan H, Lu J, Chang X, Li X, et al. Knockdown of Oct4 and Nanog expression inhibits the stemness of pancreatic cancer cells. Cancer Lett 2013;340:113–23.
31. Lee M, Nam EJ, Kim SW, Kim S, Kim JH, Kim YT. Prognostic impact of the cancer stem cell-related marker NANOG in ovarian serous carcinoma. Int J Gynecol Cancer 2012;22:1489–96.
32. Hiraga T, Ito S, Nakamura H. Cancer stem-like cell marker CD44 promotes bone metastases by enhancing tumorigenicity, cell motility, and hyaluronan production. Cancer Res 2013;73:4112–22.
33. Alizadeh AA, Eisen MB, Davis RE, Ma C, Lossos IS, Rosenwald A, et al. Distinct types of diffuse large B-cell lymphoma identified by gene expression profiling. Nature 2000;403:503–11.
34. Lee JS, Chu IS, Heo J, Calvisi DF, Sun Z, Roskams T, et al. Classification and prediction of survival in hepatocellular carcinoma by gene expression profiling. Hepatology 2004;40:667–76.
35. van `t Veer LJ, Dai H, van de Vijver MJ, He YD, Hart AA, Mao M, et al. Gene expression profiling predicts clinical outcome of breast cancer. Nature 2002;415:530–6.
36. Gu Y, Cheng Y, Song Y, Zhang Z, Deng M, Wang C, et al. MicroRNA-493 suppresses tumor growth, invasion and metastasis of lung cancer by regulating E2F1. PloS One 2014;9:e102602.
37. Alla V, Engelmann D, Niemetz A, Pahnke J, Schmidt A, Kunz M, et al. E2F1 in melanoma progression and metastasis. J Natl Cancer Inst 2010; 102:127–33.
38. Rabello DD, Lucena-Araujo AR, Alves-Silva JC, da Eira VB, de Vasconcellos MC, de Oliveira FM, et al. Overexpression of EZH2 associates with a poor prognosis in chronic lymphocytic leukemia. Blood Cells Mol Dis 2015;54:97–102.

39. Xu L, Deng Q, Pan Y, Peng M, Wang X, Song L, et al. Cancer-associated fibroblasts enhance the migration ability of ovarian cancer cells by increasing EZH2 expression. Int J Mol Med 2014;33: 91–6.
40. Fan Y, Shen B, Tan M, Mu X, Qin Y, Zhang F, et al. TGF-beta-induced upregulation of malat1 promotes bladder cancer metastasis by associating with suz12. Clin Cancer Res 2014;20:1531–41.
41. Foster CS, Falconer A, Dodson AR, Norman AR, Dennis N, Fletcher A, et al. Transcription factor E2F3 overexpressed in prostate cancer independently predicts clinical outcome. Oncogene 2004;23:5871–9.
42. Santos M, Martinez-Fernandez M, Duenas M, Garcia-Escudero R, Alfaya B, Villacampa F, et al. *In vivo* disruption of an Rb-E2F-Ezh2 signaling loop causes bladder cancer. Cancer Res 2014;74:6565–77.
43. Obinata D, Takayama K, Urano T, Murata T, Kumagai J, Fujimura T, et al. Oct1 regulates cell growth of LNCaP cells and is a prognostic factor for prostate cancer. Int J Cancer 2012;130:1021–8.
44. Borena BM, Meyer E, Chiers K, Martens A, Demeyere K, Broeckx SY, et al. Sphere-forming capacity as an enrichment strategy for epithelial-like stem cells from equine skin. Cell Physiol Biochem 2014;34:1291–303.
45. Liang X, Osman TA, Sapkota D, Neppelberg E, Lybak S, Liavaag PG, et al. Rapid adherence to collagen IV enriches for tumour initiating cells in oral cancer. Eur J Cancer 2014;50:3262–70.
46. Wang JL, Yu JP, Sun ZQ, Sun SP. Radiobiological characteristics of cancer stem cells from esophageal cancer cell lines. World J Gastroenterol 2014;20:18296–305.
47. Yamashina T, Baghdadi M, Yoneda A, Kinoshita I, Suzu S, Dosaka-Akita H, et al. Cancer stem-like cells derived from chemoresistant tumors have a unique capacity to prime tumorigenic myeloid cells. Cancer Res 2014;74: 2698–709.
48. Oshima N, Yamada Y, Nagayama S, Kawada K, Hasegawa S, Okabe H, et al. Induction of cancer stem cell properties in colon cancer cells by defined factors. PloS One 2014;9:e101735.